Ribas, I., Jordi, C., & Giménez, Á. 2000a, Monthly Notices of the RAS, 318, L55

Ribas, I., Jordi, C., Torra, J., & Giménez, Á. 2000b, Monthly Notices of the RAS, 313, 99

Saffe, C., Gómez, M., & Chavero, C. 2005, Astronomy and Astrophysics, 443, 609

Santos, N., Israelian, G., & Mayor, M. 2000, Astronomy and Astrophysics, 363, 228

Santos, N., Israelian, G., & Mayor, M. 2001, Astronomy and Astrophysics, 373, 1019

Santos, N., Israelian, G., & Mayor, M. 2004, Astronomy and Astrophysics, 415, 1153

Santos, N., Israelian, G., Mayor, M., et al. 2005, Astronomy and Astrophysics, 437, 1127

Sousa, S., Santos, N., Israelian, G., Mayor, M., & Monteiro, M. 2006, Astronomy and Astrophysics, 458, 873

Torres, G., Lacy, C., Marschall, L., Sheets, H., & Mader, J. 2006, Astrophysical Journal, 640, 1018

Vaz, A. & Vicente, L. 2007, Journal of Global Optimization, 39, 197

Yildiz, M., Yakut, K., Bakis, H., & Noels, A. 2006, Monthly Notices of the RAS, 368, 1941

J. M. Fernandes
CFC, Department of Mathematics, University of Coimbra, 3001-454 Coimbra, Portugal (jmfernan@mat.uc.pt).

A. I. F. Vaz
Department of Systems and Production, Algoritmi Research Center, University of Minho, Campus de Gualtar, 4710-057, Portugal (aivaz@dps.uminho.pt).

L. N. Vicente
CMUC, Department of Mathematics, University of Coimbra, 3001-454 Coimbra, Portugal (lnv@mat.uc.pt).

Pré-Publicações do Departamento de Matemática
Universidade de Coimbra
Preprint Number 08–50

MODELLING NEARBY FGK POPULATION I STARS: A NEW FORM OF ESTIMATING STELLAR PARAMETERS USING AN OPTIMIZATION APPROACH

J. M. FERNANDES, A. I. F. VAZ AND L. N. VICENTE

Abstract: Modelling a single star by means of theoretical stellar evolutionary tracks is a nontrivial problem due to the large number of unknowns compared to the number of observations. Currently, stellar age and mass are estimated using interpolations in grids of stellar models and/or isochrones assuming ad-hoc approximations for the mixing length parameter and the metal to helium enrichment, normally scaled on the solar values. This paper presents a new method to model the FGK main sequence of stars of Population I, capable of simultaneously estimating the following stellar parameters: mass, age, helium and metals abundance, mixing length parameter, and overshooting.

Our approach is based on the application of a global optimization method (PSwarm) to solve the inverse, simulation-based optimization models of finding the values for the stellar parameters that better match the given observations. The evaluation of the fitting function requires the simulation of a stellar evolutionary code. In these models, the helium and the mixing length are not scaled on the Sun but, together with the overshooting, considered free optimization parameters. The optimization algorithm used by PSwarm is a rigorous direct search method enriched by a population based heuristic (particle swarm) to improve the ability to search for a global optimizer.

We develop a public-domain computational tool to interface the global optimization solver and the stellar evolutionary code. We test our method using the Sun and five FGK fictitious stars and then apply our methodology to about 135 detailed spectroscopic analysed stars, including 74 planet host stars. We present and discuss the stellar parameters estimated for each star in the context of previous works. The impact of the results on stellar evolutionary studies is briefly discussed.

Keywords: optimization (global derivative-free optimization, direct search, and particle swarm), stars (fundamental parameters, Hertzsprung-Russell (HR) and C-M, and planetary systems).
AMS Subject Classification (2000): 90C90, 90C26, 90C56.

1. Introduction

The stellar evolutionary theory aims to understand how a star works and evolves. The basic idea to be achieved can be found at the seminal work of Eddington (1926) where results coming from a couple of fundamental equations

Date: October 16, 2008.

describing the interior of the stars are compared to the stellar surface observations. During all the XX century this dichotomy produced very impressive results on the knowledge of both the internal structure and the evolution of stars. A considerably part of that improvement was based on the discussion around the solar models, trying to find the best theoretical formalism that reproduces the solar radius, the bolometric luminosity, and, more recently, the helioseismoloy and the neutrinos flux for the known and observed values of the mass, the metals chemical abundance, and the age (*e.g.* Basu & Antia 2008). One of the most important outputs of this work is the extrapolation of the solar model to other stellar regimes, in particular to those of mass and chemical composition close to the solar values. Using the HIPPARCOS satellite results for a sample of 40 nearby stars, Lebreton et al. (1999) found that the same physics used in the solar model seems to be equipped to reproduce FGK stars of Population I. On the other hand, Lebreton et al. (2008), based on the preparation of COROT data, compared similar $0.9M_{\odot}$ to $5.0M_{\odot}$ stellar models produced by five different stellar evolution codes. They concluded that the differences in the global parameters (such as luminosity and effective temperature) are quite small, around 1%. So, nearby Population I FGK stars are particularly suitable (both by theoretical and observational reasons) to be modelled by means of stellar evolutionary models.

Since the discovery in 1995 of the first planet around a solar type star (Mayor & Queloz 1995), attention has been payed to the analysis of F, G, and K dwarfs. In particular, different research groups started to perform detailed spectroscopic studies of large samples of stars. The fact that planet-host stars are found to be (on the average) metal-rich when compared to field stars (e.g. Gonzalez 1997; Gonzalez et al. 2001; Santos et al. 2000, 2001, 2004; Laws et al. 2003), led to a focus on Population I stars. Furthermore, one can found analysis of a huge amount of FGK stars; see the *The N2K Consortium* (Ammons et al. 2006).

It is important to recall here that the canonical output of those spectroscopic analysis are the metallicity ($[Fe/H]$), the Effective Temperature ($T_{\rm eff}$), and the gravity (currently $log\, g$). On the other hand, most part of the analysed stars presented accurate HIPPARCOS parallaxes, and thus the Luminosity (L) can also be determined. So, thanks to the accuracy of those observations and to the large number of grids of models available in literature, it is tempting to compare or fit models to observations, in order to determine unknown stellar parameters such as the mass and the age. This is currently done using the comparisons between the stellar position in the Hertzsprung-Russel Diagram

Fernandes, J., Lebreton, Y., Baglin, A., & Morel, P. 1998, Astronomy and Astrophysics, 338, 455
Fernandes, J. & Santos, N. 2004, Astronomy and Astrophysics, 427, 607
Flower, P. 1996, Astrophysical Journal, 469, 355
Gonzalez, G. 1997, Monthly Notices of the RAS, 285, 403
Gonzalez, G., Laws, C., Tyagi, S., & Reddy, B. 2001, Astronomical Journal, 121, 432
Grevesse, N. & Noels, A. 1993, in Origin and Evolution of the Elements, ed. N. Prantzos, E. Vangioni-Flam, & M. Casse, Symposium in honour of H. Reeves (Cambridge University Press, Cambridge, England), 14–+
Henry, T. & McCarthy, D. J. 1993, Astronomical Journal, 106, 773
Houdek, G. & Rogl, J. 1996, Bulletin of the Astronomical Society of India, 24, 317
Iglesias, C. & Rogers, F. 1996, Astrophysical Journal, 464, 943
Jimenez, R., Flynn, C., MacDonald, J., & Gibson, B. 2003, Science, 299, 1552
Johnson, J., Butler, R., Marcy, G., et al. 2007, Astrophysical Journal, 670, 833
Kolda, T. G., Lewis, R. M., & Torczon, V. 2003, SIAM Review, 45, 385
Lastennet, E., Fernandes, J., Valls-Gabaud, D., & Oblak, E. 2003, Astronomy and Astrophysics, 409, 611
Laws, C., Gonzalez, G., Walker, K., et al. 2003, Astronomical Journal, 125, 2664
Lebreton, Y., Fernandes, J., & Lejeune, T. 2001, Astronomy and Astrophysics, 374, 540
Lebreton, Y., Montalbán, J., Christensen-Dalsgaard, J., Roxburgh, I., & Weiss, A. 2008, Astrophysics and Space Science, 316, 187
Lebreton, Y., Perrin, M.-N., Cayrel, R., Baglin, A., & Fernandes, J. 1999, Astronomy and Astrophysics, 350, 587
Maeder, A. & Meynet, G. 2000, Annual Review of Astronomy and Astrophysics, 38, 143
Mayor, M. & Queloz, D. 1995, Nature, 378, 355
Miglio, A. & Montalbán, J. 2005, Astronomy and Astrophysics, 441, 615
Morel, P. 1997, Astronomy and Astrophysics, Supplement, 124, 597, http://www.obs-nice.fr/cesam
Pietrinferni, A., Cassisi, S., Salaris, M., Cordier, D., & Castelli, F. 2007, in Stellar Populations as Building Blocks of Galaxies, Proceedings of IAU Symposium 241, ed. A. Vazdekis & R. Peletier (Cambridge: Cambridge University Press), 39–40

Acknowledgements. Support was provided by FCT under grants POCTI-SFA-2-675, POCI/MAT/58957/2004, POCI/MAT/59442/2004, PTDC/CTE-AST/66181/2006, and PTDC/MAT/64838/2006, and by the CDS-Strasbourg Data Base. JMF also acknowledges the support from Fundação Calouste Gulbenkian and the European Astronomical Society. We are grateful to Pierre Morel and the CESAM team to providing us the stellar evolutionary code. Finally, we would like to thank Ana Luísa Custódio (New University of Lisbon) for several interesting discussions.

References

Alexander, D. & Fergunson, J. 1994, Astrophysical Journal, 437, 879
Ammons, S. M., Robinson, S. E., Strader, J., et al. 2006, Astrophysical Journal, 638, 1004
Asplund, M. 2005, Annual Review of Astron and Astrophys, 43, 481
Basu, S. & Antia, H. M. 2008, Physics Reports, 457, 217
Bertelli, G., Girardi, L., Marigo, P., & Nasi, E. 2008, Astronomy and Astrophysics, 484, 815
Böhm-Vitense, E. 1958, Zeitschrift fuer Astrophysik, 46, 108
Casagrande, L., Flynn, C., Portinari, L., Girardi, L., & Jimenez, R. 2007, Monthly Notices of the RAS, 382, 1516
Caughlan, G. & Fowler, W. 1988, Atomic Data and Nuclear Data Tables, 40, 283
Christensen-Dalsgaard, J. 1991, in Challenges to Theories of the Structure of Moderate-Mass Stars, ed. D. Gough & J. Toomre (Springer-Verlag Berlin Heidelberg New York), 11–+
Claret, A. 2007, Astronomy and Astrophysics, 475, 1019
Conn, A. R., Scheinberg, K., & Vicente, L. N. 2008, Introduction to Derivative-Free Optimization, MPS-SIAM Series on Optimization (Philadelphia: SIAM)
Dziembowski, W., Fiorentini, G., Ricci, B., & Sienkiewicz, R. 1999, Astronomy and Astrophysics, 343, 990
Eddington, A. 1926, The Internal Constitution of the Stars (Cambridge: Cambridge University Press)
Eggenberger, P., Charbonnel, C., Talon, S., et al. 2004, Astronomy and Astrophysics, 417, 235
Eggleton, P., Faulkner, J., & Flannery, B. 1973, Astronomy and Astrophysics, 23, 325

(HRD) and theoretical stellar models (Laws et al. 2003). In the context of the exoplanets, it is clear that, at least, mass and age have a considerably impact on the theories that try to explain the formation of a star/planetary-system (e.g. Santos et al. 2004). For instance, we point out a proposed correlation between stellar mass and the probability to harbor a giant planet (Johnson et al. 2007).

The large number of these dwarfs are not in binary systems, and thus the mass can not be obtained directly by astrometry and/or spectroscopy. Moreover, age can be estimated using an empirical relation between age and stellar activity. Nevertheless this relation is also model dependent and the accuracy is not better than $20-40\%$ (*e.g.* Saffe et al. 2005). On the other hand, the authors in Fernandes & Santos (2004) studied two planet host stars (HD 37124 and HD 46375) by means of detailed stellar evolutionary models and showed that, for a fixed value of the age of these stars, uncertainties of 15% in the mixing length parameter can produce an error in the derived parameters of about 5% in mass and 20% in helium.

Let us recall also that the knowledge of the stellar HRD position is a function of the stellar mass (M), the initial individual abundance of helium (Y) and metals (Z), and the age ($t_\star$). The solution of the equations of the internal structure gives the values for $T_{\rm eff}$ and L. However, the physical inputs chosen to describe the stellar interior also constrain the evolution of the star in the HRD. In particular, some mechanisms insufficiently known, such as the convection, rotation and diffusion, are dependent of free parameters. For instance, in the framework of the Mixing Length Theory (MLT) currently used to model the stellar convection, two more (unknown) variables have to be considered: the mixing-length parameter (α) and the overshooting (ov). Thus, in order to model a star correctly we must determine all these six parameters.

Currently, the analysis on the HRD is preformed using what we can call solar-scaled stellar models. By solar-scaled stellar models, we mean models which assume solar values for those parameters lacking of strong observational constraints. This is the case for helium for which we know the minor possible value, equal to the primordial value, around 0.23, but the individual value is not available to observation in FGK dwarfs (and a similar argument applies to the mixing-length parameter). Currently, the helium abundance value in models is determined as function of the metals, assuming the same proportion Y-Z as in the Sun. This proportion is materialized by the helium-to-metals chemical enrichment parameter $\frac{\Delta Y}{\Delta Z}$ (*e.g.* Jimenez et al. 2003; Casagrande et al. 2007). The first grid of isochrones with non-solar scaled helium values has just been

published (Bertelli et al. 2008). In the case of the mixing length parameter, most parts of the grids use the same value, equal to the solar one, in all stellar models independently of the mass, the chemical composition, and the age (*e.g.* Pietrinferni et al. 2007). Concerning the overshooting, for stars of masses equal or smaller than the solar mass, it is common to consider this parameter as zero because those stars do not present a permanent convective core, and for stars of higher mass it is used a fixed value around 0.20 or 0.25.

A question which naturally arises is whether one can consider the universality and uniqueness of the mixing length parameter, the overshooting, and the helium-to-metals chemical enrichment parameter. In the last recent years a considerably amount of work has tried to answer this question.

An interesting overview about the mixing length parameter and the helium-to-metals chemical enrichment parameter is presented in Casagrande et al. (2007). From this paper, as an example, we would like to point out the results concerning the nearby visual binary star α *Centauri* and the Hyades for which it seems that the solar-scaled values for helium and the mixing length parameter are not adapted for those stars. Despite of the same chemical composition and age for both components of α *Centauri* and very similar masses ($1.1M_{\odot}$ and $0.9M_{\odot}$), the mixing length parameters are different from one component to the other and both different to the solar value (Eggenberger et al. 2004; Miglio & Montalbán 2005). Moreover, the $\frac{\Delta Y}{\Delta Z}$ founded in the binary is lower than the solar value (1.2 against 2.2 respectively). On the other hand, a detailed analysis of the main sequence of the Hyades showed that the mixing length parameter could decrease from higher to lower masses (Yildiz et al. 2006) and $\frac{\Delta Y}{\Delta Z}$ is approximately 1 (Lebreton et al. 2001). The situation for the overshooting is also puzzling. From the analysis of double-line eclipsing binary systems, Ribas et al. (2000a) suggested that the overshooting value could increase with the increase of mass. Nevertheless, more recently, Claret (2007) proposed that a single value of 0.2 could be suitable to reproduce the absolute dimensions of these kind of stellar systems.

Thus, the ad hoc hypothesis of the universality of the mixing length parameter, the overshooting, and the helium-to-metals chemical enrichment parameter should be further tested. Moreover, as stated above, the knowledge of the mass and the age is particularly relevant in the framework of the exoplanets studies. The main goal of this paper is to propose the application of a global derivative-free optimization method in order to estimate simultaneously the stellar mass, the initial individual abundance of helium and metals, the age, and the two

processor nodes). PSwarm jobs allocated 24 processors but only 22 processors were used (one master processor to run the algorithm and 21 slave processors to run as objective function evaluators). A population of 42 particles was used (twice the number of processors). While the PSwarm population was selected to be a multiple of the number of available processors, some synchronization problems can still occur (for instance, an invalid star configuration immediately detected by CESAM takes a negligible amount of time to evaluate). A wall time of 20 CPU hours was used for the 25 runs performed for each star (and rarely exceeded).

4. Discussion and conclusions

In this paper we have presented a mathematical methodology to estimate the stellar parameters (mass, age, helium and metals abundance, mixing length parameter, and overshooting) from the correspondent photometric, astrometric, and spectroscopic observations. The estimation is carried out by solving a simulation-based optimization problem using a global derivative-free algorithm. We made available to the community a computational tool to interface the global optimization solver (PSwarm) and the stellar evolutionary code (CESAM); see (1).

We tested our method in both fictitious and real FGK stars of population I. In particular, we derived, for the first time, the above stellar parameters for a sample of 135 FGK stars, including 74 planet host stars. The comparison between our quoted mass, helium and age values and those obtained previously by different authors revealed encouraging coherent results, mainly on the mass estimation. In a forthcoming paper, we plan to study in detail the impact of the derived stellar parameters on the knowledge of the chemical properties of the solar neighborhood and to make a comparison between planet host stellar population and that of stars with not planet detection. Anyway, we were able to conclude from our results (in Table 7) that the average helium abundance over the sample of planet host stars is similar to the no planet detection population, around the solar value 0.29. This is a particularly interesting conclusion as it is known that the planet host stars are, in average, more metal rich than the others. So, the metal enrichment in the solar neighborhood seems not to be followed by helium enrichment. On the other hand, the average of the age is similar in both stellar populations, around 5 Gyr. Looking over the all sample of 135 FGK stars, we did not find any clear correlation between mass and both mixing length parameter or overshooting.

TABLE 8. Comparison between the results reported by Casagrande et al. (2007) and ours.

	Obtained herein			Reported by Casagrande et al. (2007)		
HD	Age(Gyr)	Helium	Mass	Age (Gyr)	Helium	Mass
142	2.20	0.30	1.25	5.93	0.29±0.04	1.07±0.07
3651	6.18	0.30	0.88	5.13	0.21±0.06	0.97±0.10
17051	1.75	0.30	1.18	1.47	0.26±0.07	1.20±0.11
70642	5.00	0.30	1.05	3.88	0.26±0.03	1.04±0.07
130322	5.40	0.33	0.82	1.24	0.25±0.03	0.86±0.04
160691	4.80	0.30	1.17	6.41	0.29±0.03	1.08±0.06
179949	1.40	0.28	1.25	2.05	0.29±0.06	1.13±0.11
210277	5.30	0.31	1.07	6.93	0.29±0.05	0.95±0.07

To finish this section we report the average of the errors obtained in the numerical results. The average for each parameter is computed by:

$$\Delta_P^j = \frac{\sum_{i=1}^{N_j} |P_a - P_i|}{N_j}$$

where P_a is the average value reported in Table 7 and P_i is the parameter obtained at run number i. N_j is the number of runs for star j (25 when all runs were considered valid).

Typical values for Δ_P^j are (independently of j):

Δ_M	$\Delta_{t_\star}$	Δ_X
$\sim 0.05 - 0.07 M_\odot$	$\sim 1000 - 2000$Myr	$\sim 0.02 - 0.03$
Δ_Y	Δ_α	Δ_{ov}
$\sim 0.02 - 0.03$	$\sim 0.1 - 0.2$	$\sim 0.1 - 0.15$

The stellar estimation for the FGK real starts was performed in the Milipeia cluster available at the University of Coimbra. The cluster is formed by 2 management nodes (Sun Fire X4100) and 130 processor nodes (Sun Fire X4100) running the CentOS 4.4 operating system. Each node offers 2 double core processors. Since the objective function evaluation is obtained by simulating the evolution of a star, the corresponding CPU times can be significant for stars of different ages. On average each objective function evaluation takes about 1 minute. Recall that the PSwarm maximum number of objective function evaluations was set to 2000. Due to the cluster system administration, the number of requested processors must be a multiple of 4 (always allocating full

convection parameters (mixing length and overshooting), taking into account the observed metallicity, the effective temperature, the gravity, and the luminosity for each star. This optimization methodology will be applied to a sample of about 135 FGK stars issued from detailed spectroscopic analysis, including 74 planet host stars. We also provide an on-line computational tool for other researchers to use and test our methodology:

`http://www.norg.uminho.pt/aivaz/astro` (1)

This paper is organized as follows. In Section 2 we describe the input physics and optimization approach used to solve the inverse optimization model. In Section 3, we report results for the Sun and a sample of fictitious stars as well as for true FGK stars selected among those observed by Santos and co-workers. In Section 4 we discuss the results, draw conclusions, and describe the future work.

2. The estimation methodology

2.1. Input physics in stellar evolutionary models. We adjusted our estimation models especially for the stars studied in this work. The stellar evolution calculations were done using the CESAM code, version 3 (Morel 1997). In the following we present the physical ingredients used in the evolutionary code. The nuclear reactions rates are given by Caughlan & Fowler (1988). The OPAL opacities of Iglesias & Rogers (1996) are complemented at low temperatures by opacity data from Alexander & Fergunson (1994) following a prescription of Houdek & Rogl (1996). The atmosphere is described with an Eddington $T(\tau)$-law. The convection is treated according to the mixing-length theory from Böhm-Vitense (1958) leaving the mixing-length (proportional to the pressure scale height, H_p) as unknown, and thus letting α and ov be free parameters. The equation of state is the so called EFF (Eggleton et al. 1973) which is valid for solar type stars where the departure from the ideal gas is still not important. On the other hand, due to the large amount of computation taken by this work, an analytical EOS is clearly more suitable than a tabulated one. The solar mixture is taken from Grevesse & Noels (1993).

A few years ago it has been published a revision of the solar abundances of the oxygen, nitrogen, and carbon (Asplund 2005). Those abundances have a considerably effect on the total solar metallicity and the canonical value has suffered a decrease from $Z/X = 0.0245$ to $Z/X = 0.0117$. We would like to point out two results on the stellar modelling published after those revisions

where: there is a considerably disagreement between solar models with the low heavy-element abundances and helioseismology (*e.g.* Basu & Antia 2008); there are no relevant differences on the estimated age and helium of α *Centauri* for models computed with high and low Z/X value (Miglio & Montalbán 2005).

Using the solar calibration method described by Christensen-Dalsgaard (1991) and this input physics, the solar model fits, with five digits of accuracy, the observed luminosity, radius, and metallicity with $\alpha = 1.61$, helium abundance $Y = 0.279$, and $Z = 0.0173$, for the common accepted solar age of 4.6Gyr (Dziembowski et al. 1999).

We would like to point out that there are other mechanisms, not included in this work, that could affect the HRD position of a model, as the rotation (Maeder & Meynet 2000) and helium and metal gravitational settling (microscopic diffusion). However, the stars addressed in this work are slow rotators. On the other hand, diffusion has a marginal effect in the HRD position for Population I solar mass stars (*e.g.* Lastennet et al. 2003). We thus expect that the lack of these mechanisms do not considerably change our results.

2.2. The estimation model. As already stated, we consider six parameters for estimation: the stellar mass M (related to the Sun mass $M_\odot$), the abundance of hydrogen X (in percentage of the total stellar composition), the abundance of helium Y (also in percentage of the total stellar composition), the abundance of other elements Z ($Z = 1 - X - Y$), the stellar age $t_\star$ in Gyr, the stellar surface convection α, and the stellar nucleus overshooting ov.

The star evolution computational simulation is carried out by CESAM (Morel 1997) by especifying, for a given star, values for the six parameters (note that Z can be determined from the X and Y values). Among other characteristics obtained from simulation are the effective surface temperature $T_{\rm eff}$, the luminosity L, and the radius R (from which we can then obtain the stellar gravity by $g = \frac{27397M}{R^2}$).

From the observational point of view, we have an estimate for the metallicity Z/X (the relation between the abundance of other elements in relation with the hydrogen abundance), the luminosity, the effective temperature, and the gravity. For each observed parameter an absolute error is also available.

We are therefore left with four observed quantities and six unknown stellar parameters. The proposed methodology consists in the computation of the six unknown stellar parameters by solving an optimization problem whose

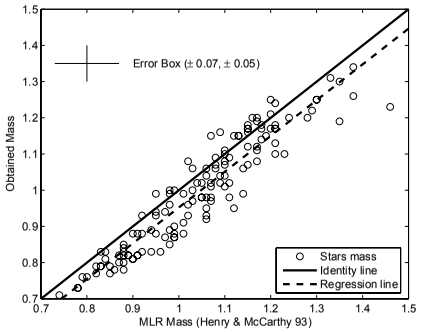

FIGURE 2. MLR results *vs* obtained mass results.

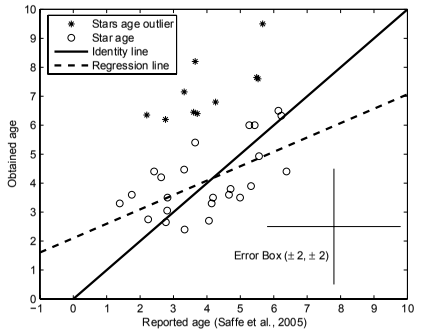

FIGURE 3. Age from Saffe et al. vs obtained age results.

A recent paper by Casagrande et al. (2007) reports numerical results on 8 stars belonging to out test set. The results published there are for the estimation of the age, helium, and mass. We report in Table 8 our obtained results versus these published ones. Casagrande et al. (2007) reports also the error associated with each star for the helium and mass. A brief analysis of Table 8 shows that the obtained results reported by us are compatible with the ones published by Casagrande et al. (2007), except for the HD130322 star. Moreover, the star HD3651 should not be included in the comparison, since we have imposed a lower bound of 0.23 for the Helium excluding from the feasible set the value reported by Casagrande et al. (2007).

Star (HD)	M ($M_\odot$)	$t_\star$ (Myr)	Y	Z	α	ov	f	Star (HD)	M ($M_\odot$)	$t_\star$ (Myr)	Y	Z	α	ov	f
43834	0.96	5248	0.30	0.0210	1.52	0.29	0.20	170493	0.76	3846	0.32	0.0226	2.00	0.28	0.17
46375	0.99	4665	0.29	0.0266	1.23	0.28	0.04	170657	0.77	4512	0.29	0.0104	1.41	0.25	0.21
50554	1.06	4262	0.29	0.0175	1.74	0.30	0.11	172051	0.85	5329	0.30	0.0104	1.42	0.23	0.29
52265	1.17	4715	0.29	0.0282	2.11	0.24	0.14	177565	1.00	5023	0.29	0.0231	1.73	0.25	0.12
53143	0.94	3713	0.30	0.0271	2.05	0.24	0.33	179949	1.25	1385	0.28	0.0282	2.11	0.30	0.30
53705	0.95	6457	0.29	0.0110	1.25	0.29	0.46	183263	1.19	4143	0.29	0.0360	2.12	0.27	0.04
57095	0.88	4661	0.28	0.0161	0.83	0.31	0.02	186427	1.04	5811	0.28	0.0207	1.61	0.19	0.39
61606	0.77	4452	0.31	0.0167	1.39	0.24	0.77	187123	1.15	3324	0.26	0.0237	1.60	0.24	0.55
65216	0.87	5898	0.30	0.0128	1.58	0.26	0.26	188015	1.16	3389	0.27	0.0344	2.04	0.27	0.35
65486	0.71	4585	0.24	0.0086	1.84	0.23	0.40	190248	1.07	6231	0.32	0.0362	1.62	0.25	0.28
67199	0.85	4751	0.29	0.0193	1.61	0.24	0.05	190360	1.09	4701	0.29	0.0294	1.45	0.28	0.22
68988	1.18	3264	0.30	0.0375	2.15	0.23	0.15	192263	0.81	5530	0.28	0.0165	1.38	0.24	0.09
70642	1.02	5036	0.30	0.0255	1.69	0.32	0.14	192310	0.83	5235	0.30	0.0162	1.18	0.27	0.76
72659	1.20	3650	0.26	0.0205	1.42	0.33	0.48	196050	1.15	4989	0.29	0.0278	1.78	0.30	0.31
72673	0.78	7639	0.26	0.0075	1.32	0.10	0.59	196761	0.83	5890	0.28	0.0089	1.24	0.18	0.24
73256	0.96	4375	0.31	0.0290	1.77	0.24	0.49	202206	1.15	2632	0.28	0.0378	2.10	0.25	0.24
73526	1.21	4622	0.28	0.0315	1.41	0.25	0.23	207129	1.01	4805	0.29	0.0171	1.69	0.25	0.44
74576	0.79	5239	0.29	0.0159	1.75	0.27	0.29	208487	1.08	4132	0.29	0.0194	1.94	0.33	0.70
75289	1.24	3262	0.28	0.0324	2.16	0.25	0.31	210277	0.98	5552	0.32	0.0248	1.31	0.29	0.62
75732	0.99	4478	0.30	0.0345	1.60	0.27	0.56	213240	1.20	4656	0.30	0.0246	1.73	0.26	0.64
76151	1.04	3791	0.29	0.0235	1.96	0.29	0.19	216770	1.00	4936	0.30	0.0300	1.57	0.23	0.18
76700	1.20	5328	0.29	0.0402	1.81	0.36	0.26	217014	1.15	4359	0.26	0.0278	1.79	0.25	0.33
82943	1.17	2822	0.30	0.0329	2.03	0.29	0.36	217107	1.07	5255	0.31	0.0368	1.68	0.16	0.38
83443	1.08	5508	0.28	0.0389	1.81	0.31	0.21	222237	0.73	4954	0.26	0.0088	1.13	0.23	0.46
84117	1.10	3797	0.29	0.0161	1.68	0.28	0.19	222335	0.81	6830	0.29	0.0117	1.30	0.23	0.60
92788	1.02	6144	0.32	0.0337	2.08	0.18	0.25	222582	1.09	3385	0.27	0.0197	1.60	0.35	0.50
100623	0.80	4075	0.25	0.0074	1.59	0.31	0.14								

In Figure 2 we present a comparison of the results obtained by the mass-luminosity relation (MLR) to our obtained numerical results. The MLR is an empirical relation than can be applied to this set of stars (see Henry & McCarthy 1993). In this figure, a filled line with slope one passing by the origin is plotted (and an exact match between the MLR results and the obtained ones would mean that all stars would be on the filled line). The dashed line represents a least squares fitting for the obtained results, showing an off-set of $0.05 M_\odot$. We point out that this MLR yields 1.055 Mo for the observed value of the solar absolute visual magnitude.

In Figure 3 we compare the ages reported by Saffe et al. (2005) to our obtained ages for about 30 stars (the ones in common with our 135 test set). The filled line represents, as in the previous figure, a line with slope one passing by the origin. Again, we can observe that the herein obtained results are generally inside the error box (except for the marked cases) and are comparable to the ones reported by Saffe et al. (2005).

objective function is the fit between the simulated and observed stellar characteristics.

2.3. The optimization formulation. Since X, Y, and Z are related by $Z = 1 - X - Y$, only two of these variables need to be consider. We have chosen to work with X and Z/X. The values for Y and Z can then be easily derived. The minimization problem is thus defined by

$$\min_{M,t_\star,X,Y,\alpha,ov} \left(\frac{T_{\rm eff} - T_{{\rm eff},obs}}{\delta T_{{\rm eff},obs}}\right)^2 + \left(\frac{L - L_{obs}}{\delta L_{obs}}\right)^2 + \left(\frac{\frac{Z}{X} - \left(\frac{Z}{X}\right)_{obs}}{\delta\left(\frac{Z}{X}\right)_{obs}}\right)^2 + \left(\frac{g - g_{obs}}{\delta g_{obs}}\right)^2 \tag{2}$$

subject to

$$(\underline{M}, \underline{t_\star}, \underline{X}, \underline{Y}, \underline{\alpha}, \underline{ov}) \leq (M, t_\star, X, Y, \alpha, ov) \leq (\overline{M}, \overline{t_\star}, \overline{X}, \overline{Y}, \overline{\alpha}, \overline{ov}), \tag{3}$$

where the subscript *obs* and the prefix *delta* denote, respectively, the observed data and the corresponding absolute errors.

Note that the objective function (2) is a nonlinear function of the optimization variables (M, $t_\star$, X, Y, α, and ov). In fact, to evaluate this function for a given set of the optimization variables the simulation must be first run. We are thus in the presence of an inverse or parameter estimation problem of the simulation-based type, for which the objective function is expensive to evaluate and its derivatives are unavailable. Our numerical experience has shown also that this problem has nonunique global minimizers. To solve this problem one must select a solver capable of doing global optimization without the use of derivatives and in a parallel environment.

Problem (2)-(3) is also an optimization problem subject to simple bounds on the variables, which can be described more generally as

$$\min_{z\in\mathbb{R}^n} f(z) \quad \text{s.t.} \quad z \in \Omega, \tag{4}$$

with

$$\Omega = \{z \in \mathbb{R}^n : \ell \leq z \leq u\},$$

where the inequalities $\ell \leq z \leq u$ are posed componentwise, $\ell \in \mathbb{R}^n$, $u \in \mathbb{R}^n$, and $\ell < u$. In this context, we have $z = (M, t_\star, X, Y, \alpha, ov)$, $\ell = (\underline{M}, \underline{t_\star}, \underline{X}, \underline{Y}, \underline{\alpha}, \underline{ov})$, and $u = (\overline{M}, \overline{t_\star}, \overline{X}, \overline{Y}, \overline{\alpha}, \overline{ov})$.

2.4. The optimization solver. The algorithm selected (PSwarm) is a direct search method enhanced by particle swarm which has been recently shown to perform well in a large variety of problems of the form (4) when compared to other global derivative-free solvers (Vaz & Vicente 2007).

Direct search methods are an important class of iterative optimization methods that try to minimize a function by comparing objective function values at a finite number of points. Direct search methods do not use derivative information of the objective function nor try to approximate it (see Conn et al. (2008); Kolda et al. (2003)). Direct search methods (of the directional type) organize their calculations at each iteration around two main steps, a poll step and a search step.

The poll step evaluates the objective function at the points in

$$P_t \;=\; \{\hat{y}(t) + \alpha(t)d,\; d \in D\}\,,$$

looking for points which have an objective function value lower than the one at the current iterate $\hat{y}(t)$. If success is attained, the value of the mesh or step size parameter $\alpha(t)$ is increased or kept constant, otherwise it is reduced. PSwarm is based on coordinate search where the positive spanning set is chosen as the maximal positive basis

$$D \;=\; D_{\oplus} \;=\; [e_1, \ldots, e_n, -e_1, \ldots, -e_n],$$

formed by the coordinate vectors and their negatives. The type of polling used in PSwarm is opportunistic in the sense that it stops once a better point is found. To handle the simple bounds on the variables one initializes the algorithm with a feasible initial guess ($\hat{y}(0) \in \Omega$) and use for polling comparisons the extreme barrier function $\hat{f}$ (instead of f itself):

$$\hat{f}(z) = \begin{cases} f(z) & \text{if } z \in \Omega, \\ +\infty & \text{otherwise.} \end{cases}$$

Given $D_{\oplus}$ and the current point $\hat{y}(t)$, one also defines a mesh

$$M_t \;=\; \left\{\hat{y}(t) + \alpha(t) D_{\oplus} z,\; z \in \mathbb{N}_0^{|D_{\oplus}|}\right\}.$$

The search step of the algorithm conducts a finite search on M_t aiming to obtain a point where the value for f is lower than $f(\hat{y}(t))$. If the search step is well succeeded, then the mesh size parameter is increased or kept constant. The poll step is only applied if the search step fails. A variety schemes can be used in the search step depending on the user purposes or problem features.

TABLE 7. FGK planet host stars: the solutions and their quality (please see text).

Star (HD)	M ($M_\odot$)	$t_\star$ (Myr)	Y	Z	α	ov	f	Star (HD)	M ($M_\odot$)	$t_\star$ (Myr)	Y	Z	α	ov	f
142	1.25	2244	0.30	0.0230	1.62	0.32	0.45	102117	1.17	4963	0.28	0.0350	1.57	0.24	0.08
1237	0.94	4056	0.30	0.0222	1.94	0.24	0.13	102365	0.93	4057	0.27	0.0095	1.27	0.29	0.70
1581	1.02	4045	0.27	0.0126	1.54	0.22	0.06	102438	0.88	4870	0.28	0.0102	1.44	0.22	0.39
2151	1.19	4504	0.29	0.0141	1.08	0.33	0.09	104304	1.06	5255	0.28	0.0312	1.80	0.30	0.36
3651	0.88	6182	0.31	0.0217	1.19	0.24	0.64	106252	0.98	6229	0.30	0.0158	1.52	0.25	0.51
4203	1.20	5094	0.30	0.0397	1.53	0.33	0.07	108147	1.17	2424	0.31	0.0259	1.97	0.31	0.49
4208	0.87	4895	0.29	0.0098	1.29	0.35	0.06	108874	1.08	6447	0.29	0.0287	1.50	0.29	0.26
4747	0.82	5867	0.28	0.0105	1.33	0.31	0.41	109200	0.78	6101	0.28	0.0100	1.17	0.23	0.14
5133	0.79	4912	0.27	0.0119	1.24	0.33	0.29	111232	0.89	4881	0.26	0.0078	1.09	0.25	0.30
7570	1.18	3000	0.29	0.0254	1.87	0.22	0.14	114729	1.10	4249	0.26	0.0101	0.86	0.29	0.58
9826	1.30	2927	0.29	0.0226	1.51	0.30	0.56	114783	0.82	5318	0.32	0.0199	1.32	0.24	0.66
10360	0.79	4775	0.27	0.0097	0.96	0.17	0.20	115617	0.91	6192	0.31	0.0169	1.37	0.33	0.66
10647	1.12	2202	0.27	0.0164	1.79	0.29	0.60	117207	1.04	5375	0.31	0.0273	1.46	0.28	0.26
10697	1.22	4179	0.30	0.0230	0.99	0.24	0.42	117618	1.12	3323	0.28	0.0198	1.63	0.29	0.37
12661	1.11	6379	0.29	0.0372	1.90	0.29	0.17	118972	0.84	4293	0.29	0.0166	1.88	0.27	0.22
13445	0.82	5000	0.27	0.0102	1.18	0.25	0.04	120136	1.31	2142	0.31	0.0275	1.65	0.33	0.22
16141	1.13	5633	0.29	0.0236	1.54	0.27	0.11	125072	0.83	3651	0.31	0.0275	1.95	0.35	0.30
17051	1.18	1750	0.30	0.0298	2.27	0.34	0.84	128311	0.83	5275	0.28	0.0185	1.20	0.26	0.33
17925	0.80	6640	0.32	0.0182	1.42	0.34	0.79	128620	1.16	3704	0.29	0.0313	1.66	0.21	0.11
19994	1.34	2811	0.30	0.0281	1.67	0.24	0.61	128621	0.93	4037	0.29	0.0254	1.48	0.26	0.48
20010	1.23	3077	0.30	0.0111	1.26	0.25	0.64	130322	0.83	5427	0.33	0.0172	1.44	0.24	0.72
20367	1.11	3705	0.31	0.0245	2.01	0.18	0.37	134987	1.15	4797	0.29	0.0333	1.74	0.26	0.25
20766	0.88	4374	0.30	0.0104	1.42	0.25	0.48	135204	0.83	6988	0.32	0.0126	0.98	0.26	0.56
20794	0.87	5247	0.26	0.0074	1.01	0.30	0.18	136118	1.26	3600	0.28	0.0159	1.57	0.27	0.89
20807	0.92	4291	0.30	0.0100	1.33	0.26	0.33	136352	0.93	4766	0.28	0.0086	1.02	0.23	0.23
21175	0.88	5672	0.30	0.0238	1.74	0.29	0.35	140901	0.99	4772	0.29	0.0228	1.86	0.28	0.17
23079	0.99	5569	0.30	0.0131	1.52	0.33	0.08	141937	1.10	2769	0.27	0.0219	1.90	0.25	0.56
23356	0.79	3530	0.29	0.0132	1.37	0.26	0.63	142022	1.02	5861	0.29	0.0258	1.39	0.32	0.29
23484	0.82	5153	0.32	0.0185	1.40	0.27	0.81	142415	1.02	3327	0.33	0.0258	2.20	0.31	0.55
23596	1.25	3650	0.32	0.0327	1.87	0.28	0.32	145675	1.00	5449	0.31	0.0389	1.54	0.27	0.30
26965	0.82	5561	0.26	0.0086	1.00	0.24	0.16	146233	1.01	4867	0.29	0.0203	1.67	0.22	0.47
28185	1.06	4534	0.29	0.0281	1.69	0.28	0.24	147513	0.98	5563	0.30	0.0198	2.07	0.27	0.08
30177	1.06	6492	0.32	0.0383	1.67	0.28	0.36	149661	0.81	6332	0.32	0.0180	1.55	0.29	0.79
30495	0.98	3682	0.30	0.0176	1.82	0.28	0.52	150689	0.73	2527	0.30	0.0140	1.77	0.27	0.69
36435	0.89	4308	0.29	0.0171	1.89	0.23	0.62	150706	0.95	5493	0.30	0.0164	2.13	0.25	0.10
38858	0.97	2501	0.26	0.0106	1.45	0.16	0.42	152391	0.88	4054	0.31	0.0178	1.83	0.31	0.03
39091	1.07	5139	0.30	0.0212	1.81	0.32	0.48	156274	0.82	5556	0.27	0.0083	1.18	0.27	0.55
40307	0.76	4138	0.26	0.0090	1.06	0.24	0.59	160691	1.17	4802	0.30	0.0340	1.68	0.32	0.09
40979	1.17	2763	0.29	0.0268	1.91	0.22	0.14	165185	0.98	4347	0.30	0.0178	1.91	0.27	0.31
41004	0.93	5667	0.30	0.0238	1.26	0.25	0.23	165499	1.14	3152	0.27	0.0180	1.38	0.27	0.04
43162	0.90	6190	0.30	0.0164	1.79	0.26	0.24	168746	0.97	4560	0.29	0.0142	1.08	0.23	0.37

we present the solutions (average for the 25 runs) for the six stellar parameters for each of the 135 stars identified by this selection procedure. Despite the fact that there are not known results for a simultaneous estimation of the six parameters, we attempt to compare our obtained results to previous results in the literature.

2003; Miglio & Montalbán 2005; Torres et al. 2006) and FGK stars in Hyades (*e.g.* Lebreton et al. 2001; Yildiz et al. 2006). Anyway, in these cases the accuracy is not higher than 0.2-0.3H_p.

- Overshooting (ov). Except for sub-solar mass models, our results show differences of about 0.1-0.2Hp. For sub-solar models (where no convective core is expected), our simulations present a nonzero value. These values must be considered as numerical results without astrophysical relevance. Double-line eclipsing binary stars are currently used to constrain the amount of overshooting. The most recent work is the one of Claret (2007) where the overshooting for individual stars is estimated with an accuracy of 0.2H_p.

The above discussion shows that our results stand in what has been recently achieved in stellar modelling by other techniques, with the advantage of being a free-parameter analysis without ad-hoc assumptions on the universality of some stellar parameters.

3.3. Real FGK stars. In this subsection we will apply the technique described above to a large sample of stars. For the choice of the observed sample, our main concern was to obtain a group of stars with spectroscopic measurements for the effective temperature, metallicity, and gravity. Ideally, the observations for each star should be made by the same technique in order to keep the internal consistency. Proximity is also a condition to include a certain star, in order to reduce the distance errors. So, we chose a sample among the FGK stars reported in Santos et al. (2004, 2005); Sousa et al. (2006). We rejected the sub-giants and those stars with error in parallaxes higher than 10% or a lack of HIPPARCOS data.

In order to apply our method we needed to compute the stellar luminosity. For that, we took the HIPPARCOS parallaxes and we assumed that the solar bolometric magnitude was 4.75 and adopted the bolometric correction in Flower (1996).

Our final sample is composed of 196 stars. As previously said, we computed 25 solutions (runs) for each star. From the 196 stars used in the numerical results we have removed from the conclusion the runs for the stars whose final objective function value was greater than 1 ($f > 1$) and those runs that lead to any variable equal to an upper or lower bound (meaning that the process may converge to another solution if the bounds were removed). After applying this filter, stars with less than 5 runs were also removed from the test set. In Table 7

In an attempt to do better global optimization, the scheme used in the search step by PSwarm is particle swarm, a well-known population based heuristic. Particle swarm tries to mimic the social behavior of a population (swarm) of individuals (particles). In the optimization context, one particle p, at time instance t, is represented by its current position $x^p(t)$, its best ever position $y^p(t)$ and a 'traveling' velocity $v^p(t)$. Let $y^p(t)$ be the best position of the particle p and $\hat{y}(t)$ represent the best particle position of the population. A new particle position is updated by

$$x^p(t+1) = x^p(t) + v^p(t+1), \tag{5}$$

where $v^p(t+1)$ is the new velocity given by

$$v_j^i(t+1) \;=\; \iota(t)v_j^i(t) + \mu\omega_{1j}(t)\left(y_j^i(t) - x_j^i(t)\right) + \nu\omega_{2j}(t)\left(\hat{y}_j(t) - x_j^i(t)\right), \tag{6}$$

for $j = 1, \ldots, n$, where $\iota(t)$ is the weighting 'inertia' factor, $\mu > 0$ is the 'cognition' parameter, and $\nu > 0$ is the 'social' parameter. The velocity vector for a given particle at a given time is thus a linear stochastic combination of the velocity in the previous time instant, of the direction to the particle's best position, and of the direction to the best swarm position (for all particles). $\omega_{1j}(t)$ and $\omega_{2j}(t)$ are random numbers drawn from the uniform $(0, 1)$ distribution. The simple bounds in the variables are handled using the orthogonal projection onto Ω.

PSwarm takes advantage of using a population in the search step to then poll at the best particle $\hat{y}(t)$, which improves the overall robustness of the population scheme. In the vicinity of a global minimizer, the application of the poll step allows the use of a reduced number of particles which is trivially achieved by dropping particles once they become too close to each other. This procedure improves the efficiency of the overall algorithm. One is able to prove (see Vaz & Vicente (2007)) that the algorithm is globally convergent to first-order stationary points and, under some additional conditions, that it can eventually meet the stopping criterion used in both search and poll steps.

2.5. Implementation details. In this section we report the modifications made in the default options and usage of PSwarm for the specific application reported in this paper. The reader is pointed to Vaz & Vicente (2007) for the default options of PSwarm and related information.

We stress that PSwarm makes a search over the variables domain regardless of their physical meaning. It is not uncommon for the simulation code (CESAM) to fail or return an unexpected result and in such cases one assigns $+\infty$ to the

objective function value (exactly as we do for infeasible trial polling points). For example, if the initial individual abundance of helium and hydrogen are not enough for a star to live until a certain given age, then CESAM code will stop at the star predicted age, and no objective function value can be computed for the specified age.

PSwarm has the capability of including any provided initial approximation in the initial randomly generated population. For the numerical results reported in this paper no initial guess was provided. In order to keep the algorithm more aggressive in the search for the global optimum, no removal of (inactive) particles from the population was performed. The search directions for the coordinate search ($D_{\oplus}$) was enriched with e (the vector of ones) and $-e$, both of the appropriate dimension. PSwarm was ran with the following parameters: 42 particles in the population, $\mu = 0.5$, $\nu = 0.5$, $\epsilon = 10^{-5}$ in the stopping criteria, and a maximum of 2000 function evaluations. The remaining parameters were left as default.

The PSwarm solver is implemented in C while CESAM is coded in Fortran 77. The major difficulty in linking the optimization solver to the simulation one was not due to the differences in the languages, but instead to the way in which CESAM ends the simulation. In fact, when CESAM terminates the simulation, achieving some form of convergence in the evolution process, it frequently does not return to the calling routine but instead exits. Thus, linking an optimization solver to CESAM causes an exit whenever an objective function evaluation is performed in these circumstances. The fix we adopted was to compute the objective function as a separate process and to use input and output files for the communication between PSwarm and CESAM. The PSwarm solver writes the values of the variables into a CESAM input file and once simulation is completed reads the objective function data from an output file. In this communication process PSwarm reads and writes the optimization variables with a limited number of significant decimal places: M uses 3 decimal places, $t_{\star}$ is an integer in Myr units (three decimal places in Gyr), X and Y are written with four decimal places, and α and ov with two decimal places. This limited accuracy is one additional difficulty posed to optimization.

3. Tests and applications

The lower and upper bounds considered in (3) are reported in Table 1. These bounds were chosen to be representative of nearby FGK Population I stars.

TABLE 6. The average over the 25 solutions for five fictitious stars in comparison with original values (in italic).

solution	M($M_{\odot}$)	$t_{\star}$(Myr)	Y	Z	α	ov	f
fake1	0.85	1600	0.2900	0.0100	1.90	0.00	
fake1	0.84	2764	0.2943	0.0100	1.99	0.34	0.17
fake2	1.30	850	0.2500	0.0300	1.00	0.25	
fake2	1.20	4270	0.2704	0.0294	1.25	0.32	0.24
fake3	1.00	5000	0.3000	0.0200	0.70	0.15	
fake3	1.00	5001	0.3057	0.0195	0.68	0.24	0.25
fake4	0.70	5000	0.3300	0.0100	2.00	0.00	
fake4	0.71	4231	0.3264	0.0103	2.00	0.28	0.04
fake5	1.10	2500	0.3600	0.0200	1.40	0.30	
fake5	1.09	3141	0.3570	0.0198	1.62	0.23	0.24

age values between the different methods is never lower than 2 to 3 Gyr. On the other hand, they also found that the internal dispersion on the isochrones method goes from 1 to 3 Gyr (see Saffe et al. 2005, Table 7). This dispersion is still marginally compatible with our difference in age for the *fake3*.

- Helium abundance (Y). Our results show a difference on helium lower than 0.025. Contrary to the previous estimations, there are not too many independent calculations of the helium for FGK stars due to the traditional lack of grids with different helium values. The most recent one is the quoted paper (Casagrande et al. 2007) which published also individual values for the helium abundance of the referred binary members and found a precision (in average) of about 0.05. A few years ago Ribas et al. (2000b) analysed a sample of 50 detached double-lined eclipsing, some of them with FGK components, by means of isochrones with non-solar scaled helium. They were able to compute individual values of helium with an accuracy of 0.04.
- Mixing length parameter. Our results show a difference on the mixing length parameter of about $0.3H_p$. To the best of our knowledge there has never been a paper published reporting computed values of the mixing length parameter for a number of stars larger than 10. Most of the calculations have been made on the context of particular objects like the Sun, binary stars (*e.g.* Fernandes et al. 1998; Lastennet et al.

TABLE 5. The 25 solutions for the fake1 fictitious star.

solution	$M(M_\odot)$	$t_\star$(Myr)	Y	Z	α	ov	f
1	0.88	4055	0.2547	0.0104	2.50	0.40	0.025
2	0.94	379	0.2290	0.0100	2.50	0.50	0.331
3	0.80	1130	0.3411	0.0091	1.43	0.42	0.106
4	0.82	102	0.3297	0.0095	1.48	0.00	0.036
5	0.86	4128	0.2751	0.0107	2.27	0.45	0.019
6	0.82	131	0.3360	0.0094	1.44	0.49	0.033
7	0.85	2148	0.2862	0.0100	1.96	0.17	0.000
8	0.83	869	0.3135	0.0094	1.61	0.41	0.015
9	0.84	213	0.3150	0.0097	1.61	0.22	0.007
10	0.91	2590	0.2326	0.0096	2.50	0.41	0.244
11	0.79	9806	0.2928	0.0102	2.28	0.50	0.141
12	0.86	4355	0.2672	0.0105	2.35	0.16	0.002
13	0.86	4504	0.2633	0.0104	2.41	0.16	0.002
14	0.77	6742	0.3323	0.0103	1.76	0.46	0.322
15	0.82	2651	0.3167	0.0101	1.74	0.49	0.051
16	0.73	6528	0.3542	0.0096	1.58	0.27	0.524
17	0.93	102	0.2497	0.0105	2.26	0.41	0.189
18	0.83	392	0.3140	0.0096	1.61	0.23	0.009
19	0.88	3383	0.2437	0.0096	2.50	0.17	0.124
20	0.71	6206	0.3775	0.0098	1.50	0.28	0.880
21	0.91	2326	0.3007	0.0190	2.50	0.44	7.648
22	0.88	100	0.2916	0.0117	2.00	0.39	0.319
23	0.80	7729	0.3120	0.0127	2.50	0.50	1.034
24	0.92	303	0.2580	0.0117	2.50	0.50	0.325
25	0.72	3484	0.4050	0.0115	1.33	0.45	1.825

12 members of spectroscopic and visual binary stars (for which the mass is very well known) achieving a precision (in average) of about $0.05M_\odot$.

- Age ($t_\star$). Except for the *fake2* the difference for the fictitious stars and for the Sun stands around or below 1 Gyr. In order to discuss this result we point to the work of Saffe et al. (2005) which compared the age of 49 planet host stars obtained by different methods: chromospheric activity, isochrones grids, lithium abundance, metallicity, and transverse velocity dispersions. The main conclusion was that the dispersion of the derived

TABLE 1. Lower and upper bounds on the variables.

	M	$t_\star$	X	Z/X	α	ov
ℓ	0.7	100	0.500	0.01	0.5	0.0
u	1.4	9999	0.761	0.06	2.5	0.5

TABLE 2. Numerical results for Sun: the estimated mass, age, helium, metals, and convection parameters.

M	$t_\star$	Y	Z	α	ov
0.991	4196	0.2915	0.0175	1.58	1.34

TABLE 3. Numerical results for Sun: retrieved solar effective temperature, luminosity, metallicity, and gravity.

Solar data	$T_{\rm eff}$	$L(L_\odot)$	Z/X
Observed ($\pm error$)	5777 (± 10)	$1.(\pm 2\times10^{-3})$	$0.0245(\pm 5\times10^{-4})$
Derived	5787	1.0046	0.0253
		$log\, g$	f
Observed ($\pm error$)		4.44 ($\pm 5\times10^{-3}$)	
Derived		4.44	3.0701

3.1. The Sun. The Sun is the natural cornerstone for modelling purposes among FGK stars. Every new stellar evolutionary code or modelling technique must be tested first using the accurate solar observation data. We apply the previous described approach to the Sun. The results are reported in Table 2 and 3, where we display the final values estimated for the parameters (M, $t_\star$, Y, Z, α, ov) and the corresponding values for $T_{\rm eff}$, L, Z/X and $log\, g$ compared to the observed ones. In Table 3 we also present the value of the objective function f (see (2)). For this computation, 2016 function evaluations were made involving 56 poll steps, out of which 31 were successful (note that since the algorithm is stochastic, different results can be obtained for different runs). See also Figure 1 for an L-shape plot representing the objective function value as a function of the number of objective function evaluations in a logarithmic scale.

The present solar results must be compared to those provided in Section 2.1. In the next section we test our algorithm for a sample of five fictitious stars. In the discussion about the astrophysical quality of the solutions obtained we

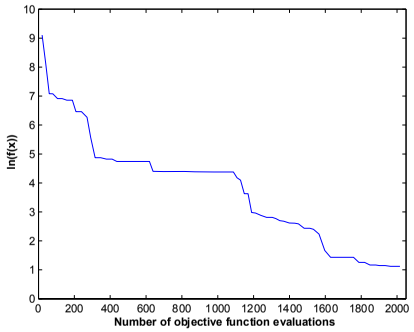

FIGURE 1. The optimization history of one run for the Sun.

TABLE 4. Fictitious FGK stars parameters ('observed' data obtained by simulation).

Star	$T_{\rm eff,obs}$	$\delta T_{\rm eff,obs}$	L_{obs}	δL_{obs}	Z/X_{obs}	$\delta Z/X_{obs}$	g_{obs}	δg_{obs}
fake1	5634	60	0.5242	0.0604	0.01429	0.005	40170	6475
fake2	5607	60	1.6967	0.1953	0.04167	0.005	18630	3003
fake3	5179	60	1.1214	0.1291	0.02900	0.005	15774	2542
fake4	5258	60	0.2941	0.0339	0.01515	0.005	44736	7211
fake5	6266	60	2.4385	0.2807	0.03230	0.005	17097	2756

will incorporate the solar results. For the moment we just point out that the solar mass is basically well reproduced. However, the estimated age is about 400 Myr lower, the helium is 0.013 higher, and the mixing length parameter is 0.3 lower. We also remark that we found a non-zero overshooting value for the Sun (without astrophysical meaning).

3.2. Fictitious FGK stars. In order to bring a supplementary test to our methodology we generated five fictitious stars using the evolutionary code CESAM for predefined values of M, $t_\star$, Y, Z, α, and ov. The correspondent values of $T_{\rm eff}$, L, Z/X, and g are those presented in Table 4. The errors (preceding by the letter δ) were chosen to be representative of nearby FGK Population I stars issued from a detailed spectroscopic analysis.

We applied our simulation-based optimization procedure (CESAM-PSwarm) to each fictitious star in order to estimate M, $t_\star$, Y, Z, α, and ov. As already

mentioned, there is no unique solution to the corresponding optimization problems. The number of parameters to be estimated is large when compared with the available observations and additional difficulties arise due to the high non-linearity of the stellar structure equations and to the use of an observational error box considered small when compared with the feasible region. To overcome this difficulty we run the simulation-based optimization 25 times (see below).

For safe of clarity, we show in Table 5, as an example, the complete set of solutions and the results on the estimated parameters M, $t_\star$, Y, Z, α, and ov for the fictitious star named *fake1*. As a first comment on this table we would like to point out that, with the exception of three cases (21, 23, and 25), all the solutions values for the objective function are lower than 1 showing a very good match of the central point of the observational error box (δL, $\delta T_{\rm eff}$, $\delta Z/X$, δg). On the other hand, the different solutions for each stellar parameter span in a considerably large range of possibilities: for instance, the mass runs between $0.72M_\odot$ and $0.94M_\odot$ and age between 100 Myr (the lower bound) and 9806 Myr. Similar comments can be made about the other parameters. Metal abundance is clearly the most 'stable' value due to the fact that $[Fe/H]$ (and so also Z/X) is an observational constraint.

We then computed the average value of all estimated values for each parameter (excluding the three referred cases where $f > 1$; see next subsection). We confirmed that after 20 runs the average did not change and, so, we chose to stop after 25 runs.

In Table 6 we present the average of the solutions for all the fictitious in comparison to the original values of M, $t_\star$, Y, Z, α, and ov. We also report the average of the objective function values which stand clearly below 1.

We analyse below the differences between the estimated values and the original ones for the fake stars as well as for the Sun (see previous section), in light of the differences reported by previous similar estimations made by other authors.

- Mass (M). The differences obtained for the mass is lower than $0.1M_\odot$. Both Santos et al. (2004) and Laws et al. (2003) have estimated the mass of FGK stars based on the interpolation of stellar evolutionary grids. The errors on these estimations are computed to be around $0.05M_\odot$. On the other hand, in this mass regime the mass-luminosity relation has an rms of about $0.07M_\odot$. Finally, Casagrande et al. (2007), using isochrones with an helium non-solar scaled, tried to recover the mass of